Article

Effects of Surface Coordination Chemistry on the Magnetic Properties of MnFeO Spinel Ferrite Nanoparticles

Christy R. Vestal, and Z. John Zhang

J. Am. Chem. Soc., **2003**, 125 (32), 9828-9833• DOI: 10.1021/ja035474n • Publication Date (Web): 18 July 2003

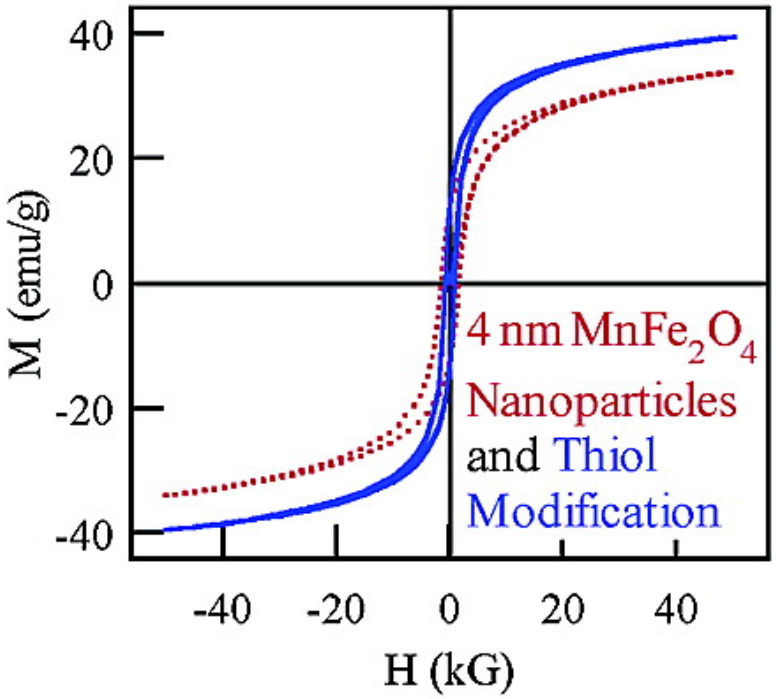

J|A|C|S
ARTICLES
Published on Web 07/18/2003

Effects of Surface Coordination Chemistry on the Magnetic Properties of $MnFe_2O_4$ Spinel Ferrite Nanoparticles

Christy R. Vestal and Z. John Zhang*

Contribution from the School of Chemistry and Biochemistry, Georgia Institute of Technology, Atlanta, Georgia 30332-0400

Received April 4, 2003; E-mail: john.zhang@chemistry.gatech.edu.

Abstract: To understand the influence of surface interactions upon the magnetic properties of magnetic nanoparticles, the surface of manganese ferrite, $MnFe_2O_4$, nanoparticles have been systematically modified with a series of *para*-substituted benzoic acid ligands ($HOOC-C_6H_4$-**R**; **R** = H, CH_3, Cl, NO_2, OH) and substituted benzene ligands (**Y**-C_6H_5, **Y** = COOH, SH, NH_2, OH, SO_3H). The coercivity of magnetic nanoparticles decreases up to almost 50% upon the coordination of the ligands on the nanoparticle surface, whereas the saturation magnetization has increased. The percentage coercivity decrease of the modified nanoparticles with respect to the native nanoparticles strongly correlates with the crystal field splitting energy (CFSE) Δ evoked by the coordination ligands. The ligand inducing largest CFSE results in the strongest effect on the coercivity of magnetic nanoparticles. The change in magnetic properties of nanoparticles also correlates with the specific coordinating functional group bound onto the nanoparticle surface. The correlations suggest the decrease in spin−orbital couplings and surface anisotropy of magnetic nanoparticles due to the surface coordination. Such surface effects clearly show the dependence on the size of nanoparticles.

Introduction

Surface chemistry is of great importance to the chemical and physical properties of nanoparticles. As the size of nanoparticles decreases, surface effects could become more significant due to the increased volume fraction of surface atoms within the whole particle. The symmetry is reduced for the chemical surroundings of magnetic metal cations at the surface due to the incomplete coordination sphere. Consequently, the magnetic structure at the surface layer usually is greatly different from that in the body of nanoparticle, and the magnetic interactions in the surface layer could have a notable effect on the magnetic properties of the nanoparticle.[1−6] Understanding the influence of surface chemistry on the magnetic properties of nanoparticles certainly facilitates our fundamental understanding of the unique magnetic behavior in nanoparticles such as the quantum origin of hysteresis in single domain magnetic nanoparticles. Furthermore, understanding and controlling the effects of surface chemistry on magnetic properties has become increasingly important for the technological applications of magnetic nanoparticles such as high density magnetic storage media, medical imaging, and drug delivery. In the information storage industry, the drive for higher density by greatly shrinking the size of data bits means surface effects become more dominant as smaller magnetic particles are employed.[7] For practical implementation in biomedical applications of nanoparticles such as magnetically guided site specific drug delivery and magnetic resonance imaging (MRI) contrast enhancement agents, the surface of the nanoparticles have to be modified with biocompatible ligands and/or polymer matrixes that also serve as drug carrying vehicles.[8,9] Once internalized, the surfaces of nanoparticles are inevitably encapsulated with biological ligands that are associated with the body's defense system.[10] Understanding the changes in magnetic behavior from these chemical interactions at surface is critical for developing magnetic nanoparticles in biomedical techniques.

Early reports on the influence of surface interactions upon the magnetic properties of nanoparticles arose from the desire to understand the role of adsorbate and metal surface interactions in catalysis. Selwood, investigating the effects of adsorbed gases such as N_2, H_2, and O_2 upon magnetic properties of Ni nanoparticles, first reported such interactions.[11] A 50% decrease on the saturation magnetization of 6.4 nm Ni nanoparticles was reported when the ratio of O_2 pressure to the weight of Ni was 60 cm^3/g at 300 K. When the adsorbate was H_2, the saturation magnetization of Ni, Ni−Si, and Ni−Cu alloy nanoparticles decreased to various extents. Compared to O_2, a ratio of 17

(1) Gradmann, U. *J. Magn. Magn. Mater.* **1991**, *100*, 481.
(2) Kachkachi, H.; Ezzir, A.; Noguès, M.; Tronc, E. *Eur. Phys. J. B.* **2000**, *14*, 681.
(3) Gazeau, F.; Bacri, J. C.; Gendron, F.; Perzynski, R.; Raikher, Y. L.; Stepanov, V. I.; Dubois, E. *J. Magn. Magn. Mater.* **1998**, *186*, 175.
(4) Kodoma, R. H.; Berkowitz, A. E.; McNiff, E. J., Jr.; Foner, S. *J. Appl. Phys.* **1997**, *81*, 5552.
(5) Spada, F. E.; Parker, F. T.; Nakakura, C. Y.; Berkowitz, A. E. *J. Magn. Magn. Mater.* **1993**, *120*, 129.
(6) Tronc, E.; Ezzir, A.; Cherkaoui, R.; Chanéac, C.; Noguès, M.; Kachkachi, H.; Fiorani, D.; Testa, A. M.; Grenèche, J. M.; Jolivet, J. P. *J. Magn. Magn. Mater.* **2000**, *221*, 63.
(7) Sugimoto, M. *J. Am. Ceram. Soc.* **1999**, *82*, 269.
(8) Mitchell, D. G. *J. Magn. Reson. Imaging.* **1997**, *7*, 1.
(9) *Scientific and Clinical Applications of Magnetic Carriers*; Häfeli, U., Schütt, W., Teller, J., Zborowski, M., Eds.; Plenum Press: New York, 1997.
(10) Davis, S. S.; Illum, L. *Biomaterials* **1988**, *9*, 110.
(11) Selwood, P. W. *Chemisorption and Magnetization*; Academic Press: New York, 1975.

10.1021/ja035474n CCC: $25.00

cm^3 H_2/g caused a 13% decrease on the saturation magnetization of Ni nanoparticles. On the other hand, the adsorption of H_2 increased the saturation magnetization of 1.5 nm Fe nanoparticles.[11] The reasons are not understood for such effects on the magnetic properties of metallic nanoparticles by gas adsorption.

The effect upon the magnetic properties of oxide nanoparticles has not been well established for ligands that are chemically bound to the particle surface. Tronc and Jolivet demonstrated that magnetic anisotropy constant of 10 nm γ-Fe_2O_3 nanoparticles changes slightly with different surface chemical treatments such as NO_3^-, ClO_4^-, and SO_4^{2-},[12] whereas Ngo et al. recently reported that the anisotropy constant of 3 nm cobalt ferrite nanoparticles coated with citrate did not change at all with respect to an uncoated sample. At the same time, the saturation magnetization decreased 9.3% after citrate coating.[13] Berkowitz et al. have compared the magnetic response of bare nanoparticles versus those with attached ligands on ~10 nm $NiFe_2O_4$ and $CoFe_2O_4$ nanoparticles. A 20% increase in saturation magnetization was observed for bare $NiFe_2O_4$ nanoparticles. However, the bare particles in these studies were prepared by annealing the coated samples at 700 °C.[14] Annealing treatments will not only remove the ligand and thus create bare particles, but may lead to increase in nanoparticle size, cation re-distribution, and "healing" effect of defects on the nanoparticle surface. Not surprisingly, the size of the $NiFe_2O_4$ nanoparticles was reported to increase from 10 to 14 nm after the thermal annealing.[14] Therefore, as Kodoma and Berkowitz et al. have pointed out later, annealing treatment complicated the direct correlations of magnetic properties to ligand surface effects.[4] Overall, the effects of surface bound ligands upon the magnetic properties are not clear and the origins of such effects certainly are not understood.

To study the effects of bound surface ligands upon the magnetic properties of nanoparticles, we prepared a series of $MnFe_2O_4$ nanoparticles with which the nature of the surface ligands was varying systematically. $MnFe_2O_4$ nanoparticles prepared by reverse micelle microemulsion methods serve as a reference and aliquots of the nanoparticles from the same batch were subsequently modified with ligands, thereby reducing errors resulting from possible batch dependent variations upon shape, cation distribution, and size. The ligands chosen for the study offer selectivity in the surface binding moiety and the "body" (the part of the ligand not involved in surface binding) components. Substituted benzoic acid ligands ($HOOC-C_6H_4$-**R**; **R** = H, CH_3, Cl, NO_2, OH) were chosen to investigate the effects due to the electron donating or withdrawing capability from the ligands with the same surface binding group (COO^-). Certainly, the dipole moment of the ligand can be tuned through the choice of the *para* R group and in fact such an approach has been used to tune the electronic properties of semiconductor surfaces.[15] To compare the effects of the binding moiety, while maintaining a consistent "body", substituted benzenes (**Y**-C_6H_5, **Y** = COOH, SH, NH_2, OH, SO_3H) were investigated. We report here the effects of these ligands on the magnetic properties of 4, 12, and 25 nm $MnFe_2O_4$ nanoparticles with emphasis on coercivity. The change on coercivity clearly correlates with the coordination chemistry features of surface bound ligands.

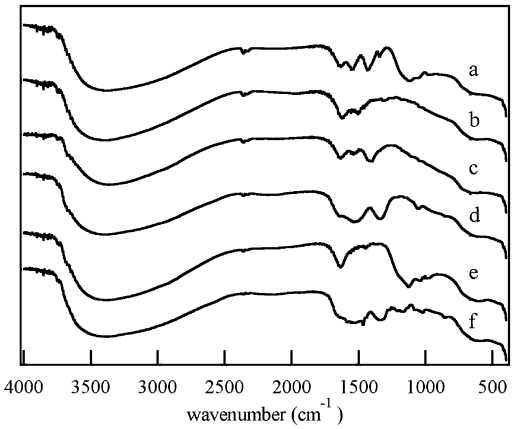

Figure 1. Spectra of surface Photoacoustic Infrared Spectroscopy (FTIR-PAS) for 4 nm $MnFe_2O_4$ nanoparticles with various ligands. The top curve is of the native 4 nm $MnFe_2O_4$ nanoparticles (a), followed by nanoparticles modified with aniline (b), benzoic acid (c), phenol (d), benzenesulfonic acid (e), and benzenethiol (f), respectively.

Experimental Section

$MnFe_2O_4$ nanoparticles were prepared by reverse micelle methods with controllable size and a size distribution less than 15%.[16] Mean sizes of 4, 12, and 25 nm $MnFe_2O_4$ nanoparticles were used in this study. Benzoic acid (Aldrich, 99%), benzenesulfonic acid (Aldrich, 90%), aniline (Aldrich, 95%), phenol (Fisher, Purified Grade), benzenethiol (Aldrich, 97%), 4-chlorobenzoic acid (Aldrich, 99%), 4-hydroxybenzoic acid (Aldrich, 99%), *p*-toluic acid (Aldrich, 98%), and 4-nitrobenzoic acid (Aldrich, 98%) were used as received. Each of these ligands were chemically bound to the nanoparticle surfaces by stirring ~20 mg $MnFe_2O_4$ nanoparticles overnight in 0.1 M ethanol solutions of the respective ligand. The nanoparticles were collected with a magnet and washed with ethanol 3−5 times to remove excess ligands. The samples were then allowed to air-dry at room temperature.

Magnetic measurements were performed with a Quantum Design MPMS-5S SQUID magnetometer. Zero-field cooled (ZFC) susceptibility measurements were performed under an applied field of 100 G. Hysteresis measurements were performed at 5 K with applied fields up to 5 T. For the hysteresis measurements, the nanoparticles were mixed with eicosane ($C_{20}H_{42}$, Aldrich) to prevent physical shifting of the nanoparticles.

Thermogravimetric analysis (TGA) and differential scanning calorimetry (DSC) were collected from room temperature to 1000 °C at a heating rate of 17 °C/min using a Netzsch Luxx STA 409 PG. Surface photoacoustic infrared spectra were collected in the frequency range of 400 to 4000 cm^{-1} using a Biorad FTS-6000 Fourier transform infrared (FTIR) spectrometer attached with a MTEC model 300 photoacoustic (PAS) detector. Transmission electron microscopy (TEM) studies were performed on a JEOL 100C operating at 100 kV.

Results and Discussion

FTIR-PAS and TGA/DSC. Figure 1 presents a series of surface photoacoustic infrared spectra (FTIR-PAS) for 4 nm $MnFe_2O_4$ nanoparticles modified with benzoic acid and benzene derivatives (Y−C_6H_5; Y = COOH, SH, NH_2, etc). Peaks corresponding to the characteristic stretching frequencies of the respective ligand are evident for each sample and clearly differ from the native $MnFe_2O_4$ nanoparticle reference. Figure 2 shows a specific example of the FTIR-PAS spectra in which the IR

(12) Tronc, E.; Jolivet, J. P. *Hyperfine Inter.* **1986**, *28*, 525.
(13) Ngo, A. T.; Bonville, P.; Pileni, M. P. *Eur. Phys. J. B.* **1999**, *9*, 583.
(14) Berkowitz, A. E.; Lahut, J. A.; VanBuren, C. E. *IEEE Trans. Magn.* **1980**, *MAG-16*, 184.
(15) Ashkenasy, G.; Cahen, D.; Cohen, R.; Shanzer, A.; Vilan, A. *Acc. Chem. Res.* **2002**, *35*, 121.
(16) Liu, C.; Zou, B.; Rondinone, A. J.; Zhang, Z. J. *J. Phys. Chem. B* **2000**, *104*, 1141.

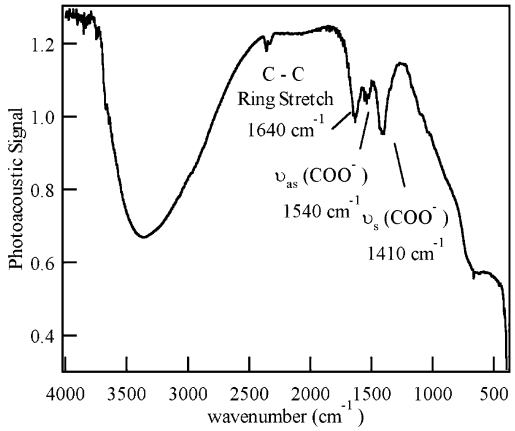

Figure 2. FTIR-PAS spectra of 4 nm $MnFe_2O_4$ nanoparticles modified with benzoic acid.

stretching frequencies from ligand-modified $MnFe_2O_4$ nanoparticles are identified for benzoic acid ligand. Strong bands at 1640 and 1410 cm^{-1} result from the skeleton C−C vibrations of the benzene ring and the symmetric carboxyl COO^- stretch, respectively. A weak band at 1540 cm^{-1} indicates the asymmetric carboxyl COO^- stretch. However, the C═O stretching frequency of the parent benzoic acid ligand usually at ∼1700 cm^{-1} is not observed in the spectrum. Such a disappearance of the C═O stretching band has been observed in *p*-nitrobenzoic acid adsorbed onto silver; benzoic acid, *m*-hydroxy benzoic acid, or *p*-hydroxybenzoic acid adsorbed onto stainless steel; and benzoic acid onto α-FeOOH.[17−19] The disappearance has been suggested to result from the surface binding of the ligands through the COOH group by release of a proton. The lack of a band at 1700 cm^{-1} in our spectra of benzoic acid derivatives is thereby attributed to the benzoic acid ligand chemically bound to the nanoparticle surface through the COO^- functionality. Similar results of missing and/or distorted bands comparable to literature reports for adsorbed aniline and/or benzenethiol are observed. These results indicate that the ligands indeed are chemically bound to the nanoparticle surface.[20,21] Comparison studies by TEM analysis before and after surface modification have shown that the nanoparticle size is not reduced, which indicates that there is no possible dissolving of surface layers during the surface modification processes.

TGA and DSC studies have been carried out for the nanoparticles modified with various ligands. Each ligand modification case gives its distinctive TGA and DSC curves, which certainly indicates that the respective ligands are truly bound onto the surface of nanoparticles in contrast with the ligands simply depositing onto the surface. As representative examples, Figure 3 shows the TGA and DSC curves of nanoparticles modified with benzenethiol and benzenesulfonic acid. Because the size of nanoparticles and the molecular weight of ligands are well defined, the grafting density of the ligands on nanoparticle surface can be estimated from the TGA/DSC data. Table 1 lists the grafting density of representative ligands

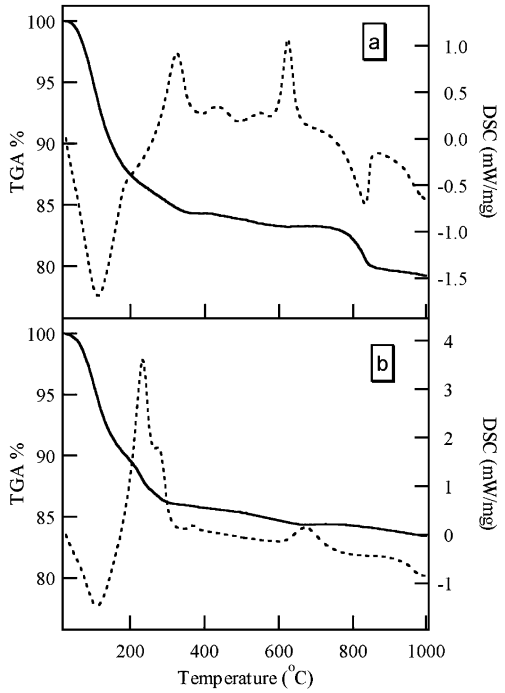

Figure 3. TGA (solid line) and DSC (dashed line) curves for (a) benzenesulfonic acid modified 4 nm $MnFe_2O_4$ nanoparticles and (b) benzenethiol modified nanoparticles.

Table 1. Grafting Density of Selected Ligands on Surface of $MnFe_2O_4$ Nanoparticles Determined from TGA/DSC Data

ligand	grafting density (molecules/nm^2)
benzoic acid	1.20
p- toluic acid	1.39
p − hydroxybenzoic acid	1.40
benzenethiol	1.29
aniline	1.52
benzenesulfonic acid	1.26
phenol	1.19

determined from the TGA/DSC data. These results are in good agreement with the literature data of benzoic acid derivatives adsorbed onto micron size particles of stainless steel. For instance, the grafting density was 1.17, 1.16, and 1.28 molecules/nm^2 on 8−10 μm stainless steel particles for benzoic acid, *m*-hydroxybenzoic acid, and *p*-hydroxybenzoic acid, respectively.[18] Furthermore, Table 1 clearly shows that the grating density on our nanoparticle surface is comparable among all the surface modification ligands that we have used. The comparable grafting density allows for meaningful comparisons among various surface-coordinating ligands. Vastly differing coverage density would represent different surface environments and therefore will introduce uncertainty to the magnetic response of nanoparticles after the surface modification.

Magnetic Properties. Zero field cooled (ZFC) susceptibility measurements reveal that the blocking temperature, T_B, of the native nanoparticles and the ligand modified nanoparticles remains as a constant of ∼20 K without any change beyond experimental error. However, the hysteresis measurements show unmistakable changes upon surface coordination of ligands. Figure 4 shows a typical hysteresis measurement at 5 K for native 4 nm $MnFe_2O_4$ nanoparticles and the same nanoparticles modified with benzoic acid. Upon coating with benzoic acid, the coercivity of the particles is reduced. At the same time, the

(17) Osawa, M.; Ataka, K.; Yoshii, K.; Nishizawa, Y. *Appl. Spectrosc.* **1993**, *47*, 1497.
(18) Suzuki, O.; Shibata, Y.; Inove, M. *J. Colloid Interface Sci.* **1997**, *193*, 234.
(19) Tejedor-Tejedor, M. I.; Yost, E. C.; Anderson, M. A. *Langmuir* **1990**, *6*, 979.
(20) Tanaka, M.; Ogasawana, S. *J. Catalysis* **1972**, *25*, 111.
(21) Fauconnier, N.; Pons, J. N.; Roger, J.; Bee, A. *J. Colloid Interface Sci.* **1997**, *194*, 427.

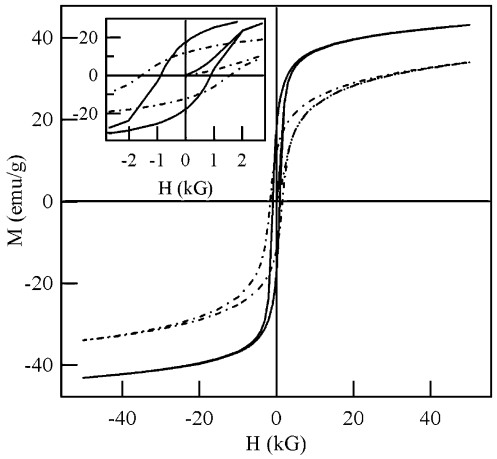

Figure 4. Field dependent magnetization at 5 K for native 4 nm $MnFe_2O_4$ nanoparticles (dashed lines) and 4 nm $MnFe_2O_4$ nanoparticles modified with benzoic acid (solid lines). Insert shows the coercivity in detail.

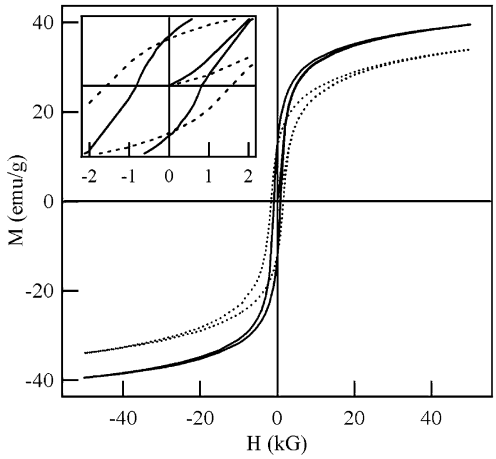

Figure 5. Hysteresis curve at 5 K for native 4 nm $MnFe_2O_4$ nanoparticles (dashed lines) and 4 nm $MnFe_2O_4$ nanoparticles modified with benzenethiol (solid line). Insert shows the coercivity in detail.

Table 2. Percentage Decrease in Coercivity from Surface Modification by *para* Substituted Benzoic Acid Ligands with Respect to the Native 4 nm $MnFe_2O_4$ Nanoparticles

ligand	pK_a	H_C (G)	% H_C decrease
native 4 nm $MnFe_2O_4$		1563	
$p-$ hydroxybenzoic acid (**R** = OH)	4.48	808	48.3
$p-$ toluic acid (**R** = CH_3)	4.27	871	44.3
benzoic acid (**R** = H)	4.19	885	43.4
$p-$ chlorobenzoic acid (**R** = Cl)	3.98	975	37.6
$p-$ nitrobenzoic acid (**R** = NO_2)	3.42	1058	32.3

Table 3. Percentage Decrease in Coercivity from Surface Modification by Benzene Derivatives with Respect to the Native 4 nm $MnFe_2O_4$ Nanoparticles

ligand	H_C (G)	% H_C decrease
native 4 nm $MnFe_2O_4$	1563	
benzenethiol (**Y** = SH)	814	47.9
benzoic acid (**Y** = COOH)	885	43.4
benzenesulfonic acid (**Y** = SO_3H)	1005	35.7
aniline (**Y** = NH_2)	1091	30.2
phenol (**Y** = OH)	1171	25.1

addition of benzoic acid to the nanoparticle surface increases the saturation magnetization. Table 2 lists the benzoic acid ligands with various para substitutants and the percentage coercivity decrease of the modified $MnFe_2O_4$ nanoparticles with respect to the coercivity of the native nanoparticles. The experimental error in terms of reproducibility in coercivity measurement is $\pm 2\%$. It is clear from Table 2 that the coercivity of nanoparticles decreases after surface coordination by modification ligands. Furthermore, the percentage coercivity decrease gets smaller as the pK_a of the ligand decreases.

The nature of the moiety bound to the surface was also found to influence the hysteresis behavior of the nanoparticles. Figure 5 shows an example of the hysteresis measurements, in which benzenethiol is attached to the surface of 4 nm $MnFe_2O_4$ nanoparticles. Like the substituted benzoic acid ligand series, the coercivity decreased and the saturation magnetization increased upon coating with various substituted benzene ligands. Table 3 lists the percentage coercivity decrease with respect to the native 4 nm $MnFe_2O_4$ nanoparticles due to the results of attaching benzenes derivatives on surface. The choice of functional group bound to the surface clearly results in distinctive differences in the magnitude of the coercivity changes.

Similar results are observed for the hysteresis behavior of 12 and 25 nm $MnFe_2O_4$ nanoparticles with blocking temperatures as 210 and 515 K, respectively. The influence on coercivity from representative ligands is listed in Table 4 for the three sizes of $MnFe_2O_4$ nanoparticles. Clearly, each ligand evokes a different response in the magnitude of coercivity decrease for each of the three sized nanoparticles. In addition, as the nanoparticle size increases, the percentage coercivity decrease from a particular ligand is getting smaller. The magnitude of percentage coercivity decrease for the 12 and 25 nm $MnFe_2O_4$

Table 4. Percentage Decrease in Coercivity of Variable Sized Modified Nanoparticles with Respect to the Corresponding Native 4, 12, and 25 nm $MnFe_2O_4$ Nanoparticles

	4 nm $MnFe_2O_4$		12 nm $MnFe_2O_4$		25 nm $MnFe_2O_4$	
ligand	H_C (G)	% H_C decrease	H_C (G)	% H_C decrease	H_C (G)	% H_C decrease
native $MnFe_2O_4$	1563		799		354	
$p-$ hydroxybenzoic acid	808	48.3	678	15.2	310	12.4
p- toluic acid	871	44.3	690	13.6	313	11.5
benzenesulfonic acid	1005	35.7	598	25.1	301	15.0
aniline	1091	30.2	602	24.7	314	11.3
phenol	1171	25.1	767	4.0	345	2.5

nanoparticles coated with the benzene derivative ligand series follows the same trend as the 4 nm nanoparticles. The correlation between pK_a and percentage decrease observed for the substituted benzoic acid series in the larger sized nanoparticles is not as clear as the correlation in using 4 nm $MnFe_2O_4$ nanoparticles. The coercivity does decrease upon coating with these ligands; nevertheless, the percentage of coercivity decrease among all the ligands does not change as much as in smaller nanoparticles and does not clearly follow the pK_a values.

The observed decrease in coercivity of $MnFe_2O_4$ nanoparticles after a series of ligands are attached onto their surface is consistent with a reduction in the surface magnetic anisotropy of nanoparticles. Although the oxygen coordination for metal cations in $MnFe_2O_4$ spinel is highly symmetrical in the forms of tetrahedron and octahedron, the coordination symmetry is greatly reduced for metal cations at the surface due to missing of some coordination oxygen atoms. Consequently, the magnetic structure at the surface layer could be drastically different than

the one in the core of spinel nanoparticles. Surface usually exhibits some degree of spin disorder and pinning. Qualitatively, adsorbed ligands can be viewed as effectively taking the positions of the missing oxygen atoms, which makes the symmetry and crystal field of the surface metal ion more closely resembling that of the core, and therefore reduces the spin disorder and pinning. Such changes certain affect the surface anisotropy and consequently the coercivity of nanoparticles. Certainly, it is inadequate to attribute coercivity of nanoparticles only to the magnetocrystalline anisotropy as in the Stoner−Wohlfarth model.[22] In 1954, Néel added the surface anisotropy to account for the effects of symmetry reduction at nanoparticle surfaces upon spin−orbit couplings.[23] Néel's early calculations as well as several recent theoretical studies have suggested that coercivity decreases with decreasing surface anisotropy.[23−25]

The observed increase in the saturation magnetization in all of our nanoparticulate samples can also be considered in terms of reducing surface anisotropy. Surface anisotropy is often pictorially viewed in terms of the degree of spin disorder and/or spin pinning at the surface. It appears that coating the surface with the ligands "frees" the surface spins, and hence, they are more easily able to align with the overall magnetization direction of the nanoparticle. As a result of such increasing alignment, the magnetization of nanoparticles is observed to increase after surface modification. Contrary to our findings, Ngo, et al. reported a decrease in saturation magnetization upon coating cobalt ferrite nanoparticles with citrate,[13] whereas Spada, et al. reported no change in saturation magnetization in polyphosphate treated γ-Fe_2O_3.[5] The reasons for such discrepancies in the studies of saturation magnetization are not entirely clear. However, it is worth while to notice the differences in the nanoparticulate samples used in these studies. Ngo, et al. reported a change in the chemical composition of the $CoFe_2O_4$ nanoparticles after the surface modification, which was attributed to preferentially dissolving Co cations from the surface layer in the modification process and implied a completely different surface generated after the surface modification. In the studies by Spada et al., the samples were acircular with a size of ∼23 nm by ∼200 nm. Certainly, the surface atoms and therefore surface effects are much less dominant in the samples with such sizes.

Although interparticle interactions contribute to the magnetic responses observed in our nanoparticles, the differences in magnetic response from various modified nanoparticles cannot be attributed to the possible variation of interparticle interactions because of the similar size, shape, and grafting density of the ligand series chosen for this study. If the body of the ligands were allowed to vary in length, certainly interparticle separation factors should be considered.

For both ligand series presented here, a correlation can be established between the percentage coercivity decrease of 4 nm $MnFe_2O_4$ nanoparticles and the crystal field splitting energy of the coordination ligands at the particle surface. When the surfaces of magnetic nanoparticles were coordinated by *para* -substituted benzoic acid ligand series (Table 2), the largest decrease in coercivity occurred with ligands having higher pK_a values. The great advantage of utilizing substituted benzoic acid ligands is from the existing correlation between the pK_a value of the ligand and the electron withdrawing/donating effects possessed by the R-substituent. The more electron donating the R-substituent is, the higher the pK_a value. As pK_a values increase, the substituted benzoic acid ligands become weaker acids.

Scheme 1

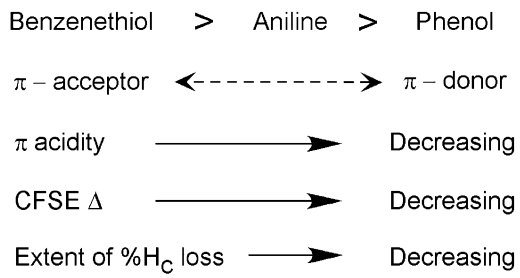

Upon the basis of ligand field theory, the ligand coordination provides the crystal field splitting energy (CFSE) Δ generated from *d* orbitals splitting with a magnitude determined by the ligands at a given coordination symmetry. As a ligand becomes more basic, the strength of the metal−ligand σ bond increases, and consequently CFSE Δ associated with the ligand increases.[26] As the pK_a of the ligands increases in *para* -substituted benzoic acid ligand series, the CFSE Δ induced by those ligands is expected to increase. Therefore, the trend in percentage decrease of coercivity with increasing pK_a of substituted benzoic acid ligands corresponds to the increase of CFSE Δ associated with the ligands that have coordinated onto the surface of the magnetic nanoparticles.

The acidity of the coordination ligands is a major factor when different functional groups are chosen for the binding moiety onto the surface of the nanoparticles (Table 3). Using different binding group onto surface could be a little more complicated since different binding modes are likely present at the particle surface. For example, benzoic acid has been proposed in numerous reports to bind via chelation to surface cations.[18−19,27−28] However, the nonchelating ligands of benzenethiol, aniline, and phenol offer a straightforward comparison in the ligand π-acidity and CFSE Δ. Benzenethiol is a stronger π-acceptor than aniline, while phenol is a weak π-acceptor, but a strong π-donor.[29] In ligand field theory, it is well established that π-acceptors result in larger CFSE Δ than π-donors.[26] Because of the π-acidity of ligands, CFSE decreases in the order of benzenethiol, aniline, and phenol. $MnFe_2O_4$ nanoparticles with benzenethiol as surface coordination ligand shows the largest coercivity decrease followed by aniline, then phenol in agreement with the decreasing CFSE Δ in these ligands. Such correlations are depicted in Scheme 1.

In both coordination ligand series, the largest percentage decrease in coercivity is displayed in the nanoparticles with a surface coordinated by the ligands that evoke the biggest CFSE Δ. As ligand field theory has indicated, the transition metal

(22) Stoner, E. C.; Wohlfarth, E. P. *Philos. Trans. R. Soc. A* **1948**, *240*, 599; reprinted in *IEEE Trans. Magn.* **1991**, *27*, 3475.
(23) Néel, L. *J. Phys. Radium* **1954**, *15*, 225.
(24) Dimitrov, D. A.; Wysin, G. M. *Phys. Rev. B* **1994**, *50*, 3077.
(25) Kodoma, R. H.; Berkowitz, A. E. *Phys. Rev. B* **1999**, *59*, 6321.
(26) Figgis, B. N.; Hitchman, M. A. *Ligand Field Theory and Its Applications*; Wiley-VCH: New York, 2000.
(27) Evanko, C. R.; Dzombak, D. A. *J. Colloid Interface Sci.* **1999**, *214*, 189.
(28) Fauconnier, N.; Bee, A.; Roger, J.; Pons, J. N. *J. Molecular Liq.* **1999**, *83*, 233.
(29) Huheey, J. E.; Keiter, E. A.; Keiter, R. L. *Inorganic Chemistry: Principles of Structure and Reactivity*, 4th ed.; HarperCollins College Publishers: New York, 1993. p 431.

having a larger d orbital energy level splitting due to ligand coordination should have a smaller spin−orbit coupling parameter ξ, which measures the interaction strength of the spin and orbital angular momentum.[26] Magnetic anisotropy is generated by the spin−orbital couplings occurred at magnetic cations, and the anisotropy decreases with decreasing spin−orbital coupling.[30] When the metal cations at the surface layer of nanoparticles are coordinated with ligands, the spin−orbital coupling is reduced, and consequently the surface anisotropy decreases and the coercivity of nanoparticles is reduced. As the CFSE Δ resulted by the ligand gets larger, the spin−orbital coupling ξ becomes smaller. Therefore, the surface anisotropy is reduced further and the coercivity H_C becomes even less. The magnetic anisotropy in nanoparticles includes the anisotropy in the core and the surface anisotropy. The results here indicate that the blocking temperature of magnetic nanoparticles is predominately determined by the magnetic anisotropy in the core, while the surface anisotropy mainly has the effect on coercivity of nanoparticles. Certainly, the extent of the surface anisotropy effect shown here is astonishingly strong on magnetic coercivity.

The effects of percentage coercivity loss as a function of nanoparticle size (Table 4) are consistent with surface effects. For 4 nm nanoparticles, surface atoms make up ~50% of the total volume of atoms and therefore contribute to the net magnetic response to a large degree. The volume fraction of atoms at the surface is reduced as nanoparticle size increases. As a result, the influence of atoms at the surface does not contribute to the total magnetic response of larger nanoparticles as strongly as to 4 nm nanoparticles. Hence for the same ligand, the coercivity does not decrease as dramatically when the size of nanoparticles is increased. The loss of a clear correlation between the pK_a of substituted benzoic acid ligands and the coercivity decrease in 12 nm and 25 nm nanoparticulate samples may be attributed to the fact that the changes in surface coordination bonding evoked by changing the *para* substituent are quite subtle. At larger nanoparticle sizes, the overall surface influences are greatly weakened, and therefore these slight variations may not be observable. When the electronic nature of the binding moiety is more markedly changed, as in the case of the benzene derivatives in which the atom attached to the surface is different, the electronic effects are likely stronger, and hence, the variations in surface effects on the magnetic properties are still able to be observed in larger nanoparticles.

(30) Liu, C.; Zou, B.; Rondinone, A. J.; Zhang, Z. J. *J. Am. Chem. Soc*. **2000**, *122*, 6263.

Conclusions

Three sizes of $MnFe_2O_4$ nanoparticles have been modified with a series of substituted benzoic acid and substituted benzene ligands. In all cases, the coercivity was found to decrease and the saturation magnetization increase upon coating with the ligand. Furthermore, a correlation between the nature of the bound surface ligand and magnetic response has been demonstrated. In both ligand series, the maximum coercive loss was found in nanoparticles modified with a surface coordination ligand that is able to evoke a larger degree of crystal field splitting energy. The extent of coercivity decrease correlates with the capability of inducing crystal field splitting energy by surface coordination ligand. Such correlations can be understood from the fact that the spin−orbit couplings of magnetic cations decrease with increasing crystal field splitting energy evoked by the coordination ligands. Certainly, the magnetic response of nanoparticles to the surface modification elucidates the quantum origins of magnetic properties such as hysteresis. Furthermore, the effects of surface coordination chemistry upon the magnetic nanoparticles are important for the design of magnetoelectronic devices that make use of spin exchange at surfaces. The surface effects should also have impacts on the potential use of surface magnetism for tuning the magnetic properties of nanoparticles, and on the development of bioligand-modified magnetic nanoparticles for biomedical applications.

Acknowledgment. C. R. V. is partially supported by a Georgia Tech Presidential Fellowship. We thank Dr. Chris Jones and his laboratory for use of the DSC/TGA, and Dr. Art Janta and Mr. Anthony Smith for use of the PAS-IR. TEM studies were performed at the Georgia Tech Electron Microscopy Center. This research is supported in part by NSF (DMR-9875892), Sandia National Laboratory, and PECASE Program.

JA035474N